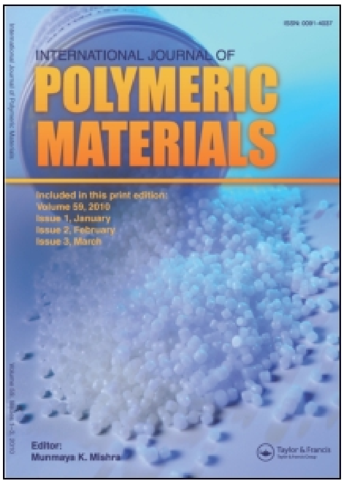

International Journal of Polymeric Materials
Publication details, including instructions for authors and subscription information:
http://www.informaworld.com/smpp/title~content=t713647664

Terpolymer Chelates: Synthesis, Characterization, and Biological Applications

Mohamed A. Riswan Ahamed[a]; Raja S. Azarudeen[a]; Duraisamy Jeyakumar[b]; Abdul R. Burkanudeen[a]
[a] PG and Research Department of Chemistry, Jamal Mohamed College (Autonomous), Tiruchirappalli, Tamil Nadu, India [b] Functional Materials Division, Central Electrochemical Research Institute, Karaikudi, Tamil Nadu, India

To cite this Article Riswan Ahamed, Mohamed A. , Azarudeen, Raja S. , Jeyakumar, Duraisamy and Burkanudeen, Abdul R.(2011) 'Terpolymer Chelates: Synthesis, Characterization, and Biological Applications', International Journal of Polymeric Materials, 60: 2, 124 — 143

To link to this Article: DOI: 10.1080/00914037.2010.504165

URL: http://dx.doi.org/10.1080/00914037.2010.504165

International Journal of Polymeric Materials, 60:124–143, 2011
Copyright © Taylor & Francis Group, LLC
ISSN: 0091-4037 print/1563-535X online
DOI: 10.1080/00914037.2010.504165

Terpolymer Chelates: Synthesis, Characterization, and Biological Applications

Mohamed A. Riswan Ahamed,[1] Raja S. Azarudeen,[1]
Duraisamy Jeyakumar,[2] and Abdul R. Burkanudeen[1]

[1]PG and Research Department of Chemistry, Jamal Mohamed College (Autonomous), Tiruchirappalli, Tamil Nadu, India
[2]Functional Materials Division, Central Electrochemical Research Institute, Karaikudi, Tamil Nadu, India

Terpolymer ligand was synthesized from 8-hydroxyquinoline and anthranilic acid with formaldehyde (QAF) by solution condensation in an acid medium. Polychelates of Cu(II), Ni(II), Zn(II), and Pb(II) were prepared using the terpolymer as ligand. The ligand and chelates were characterized by elemental analysis, TGA, DSC, FTIR, electronic absorption, and NMR spectroscopy. The activation energy was calculated for the ligand and its polychelates formation by the Freeman-Carroll method. The ligand and its polychelates possess antimicrobial activity for certain bacteria such as *Staphylococcus aureus, Escherichia coli*, and fungi *Aspergillus niger* and *Candida albicans*. The surface morphology of the ligand and its polychelates was established by SEM.

Keywords antimicrobial screening, morphology, polychelates, polycondensation, thermogravimetric analysis

INTRODUCTION

Polychelates possess attractive applications for environmental pollution control, bioinorganic catalysts, hydrometallurgy, semiconducting devices, and metal recovery from dilute solutions [1–5]. Poly(acrylic acid-*co*-maleic acid) forms complexes with Cu(II), Ni(II) and Co(II) and its good conductivity and

---

Received 14 March 2010; accepted 2 June 2010.
The authors thank the Management and Principal of Jamal Mohamed College, Tiruchirappalli, Tamil Nadu for their support and encouragement.
Address correspondence to Abdul R. Burkanudeen, PG and Research Department of Chemistry, Jamal Mohamed College (Autonomous), Tiruchirappalli, Tamil Nadu, India. E-mail: a_deen@rediffmail.com

thermal stability has been reported [6]. Salicylaldehyde oligomer–metal complexes demonstrated high stability against thermooxidative degradation, and the half degradation temperature of Zn(II) and Co(II) complexes are higher than that of the ligand [7]. Based on X-ray diffraction studies, the Cu(II) and Ni(II) complexes of poly(3-acetyl-4-hydroxyphenyl acrylate) were crystalline against its ligand [8]. Co(II), Ni(II) and Cu(II) metal complexes of bis(3-acetylcoumarin) thiocarbohydrazone have promising cytotoxic activity and antimicrobial activity [9]. The novel and simple layer-by-layer chemical deposition method was adopted for the preparation of nano-sized 8-hydroxyquinolate complexes [10]. Coordination polymers were synthesized and reported for their interesting complexation behavior with few transition metals and lanthanides [11,12]. Polymer-metal complexes of copper(II) and nickel(II) derived from poly(2-hydroxy-4-(meth)acryloxyacetophenoneoxime) were found to have good thermal stability and poor conductivity [13]. Ln(III) polymer-metal complexes were used as eco-friendly catalysts for the synthesis of 3,4-dihydropyrimidin-2(1H)-ones [14]. Chelate polymers involving azelaoyl bis-N-phenyl hydroxamic acid possess tetrahedral geometry for Mn(II) and Zn(II) and octahedral geometry for Ni(II) and Co(II) [15]. 8-hydroxyquinoline and its derivatives have been synthesized and reported for their good binding capacity with transition and post-transition metals [16]. Chelates of poly[maleic anhydride-alt-acrylic acid] copolymer were prepared and reported for their good thermal stability [17]. A copolymer involving 2,4-dichlorophenylmethacrylate and vinyl acetate was reported as a significant inhibitor for the growth of microorganisms [18].

This research article describes the synthesis of QAF ligand and a few of its polychelates. Further, the characterization and biological applications for the ligand and its chelates were carried out and reported.

EXPERIMENTAL

Materials

All chemicals used were of AR grade. The solvents were used after distillation.

Synthesis of Terpolymer Ligand

The ligand was synthesized by the refluxation of 8-hydroxyquinoline (0.1 mol) with anthranilic acid (0.1 mol) and formaldehyde (0.2 mol) in glacial acetic acid medium at $160 \pm 2°C$ for 6 h. After the specified time, the reaction mixture was cooled, poured into crushed ice with constant stirring and left overnight. The dark brown-colored resin was separated out. The unreacted

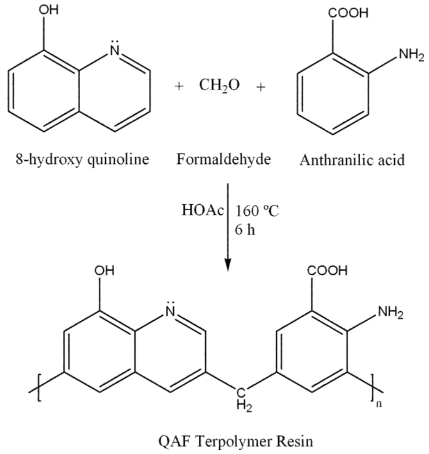

Scheme 1: Reaction sequence for the synthesis of terpolymer ligand.

monomers were removed by repeated washing with warm water, methanol, and ether and dried. It is then dissolved in 8% NaOH and regenerated using 1:1(v/v) HCl/water and cured in an air oven at 75°C for 24 h. The yield of the terpolymer ligand was found to be 75%, and the reaction sequence for the synthesis is shown in Scheme 1.

Preparation of Polychelates

The polymeric ligand (0.1 mol) was dissolved in DMSO and the metal nitrates (0.05 mol) of Cu(II), Ni(II), Zn(II), and Pb(II) were dissolved in methanol separately and filtered off. The resultant solutions were mixed together with constant stirring and refluxed for 3 h. The polychelates obtained were separated and washed with ether and methanol. Furthermore, the polychelates were dried in an air oven at 40°C for 24 h. The reaction scheme for the preparation of the polychelates is shown in Scheme 2.

Viscometric Measurements

The viscosity-average molecular weight of the terpolymeric ligand was determined using a Brooke Field viscometer (Model DV-II+) in DMSO solvent. By selecting the appropriate spindle and adjusting the spindle speed, the viscosity-average molecular weight of the ligand was calculated by multiplying the value obtained in the viscometer and its spindle number. The experiment was repeated twice to confirm the viscosity-average molecular weight of the terpolymer.

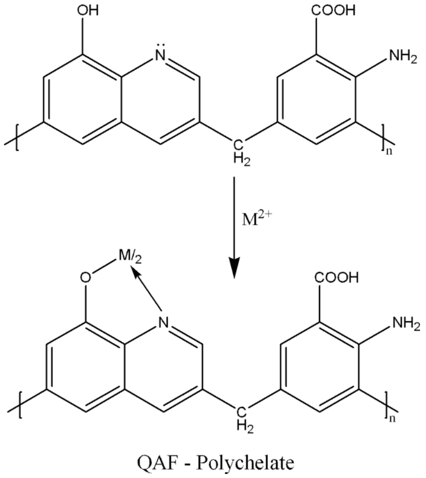

Scheme 2: Preparation route for the polychelates.

Spectral Analysis

The FTIR spectrum of the synthesized ligand and its polychelates had been scanned in KBr pellets on a Bruker (Model Tensor 27) spectrophotometer to identify the linkages and the functional groups. The UV-visible spectrum of the ligand and polychelates was recorded in a Cary Eclipse Varian instrument (Model U 3400) spectrophotometer, and the ^{1}H NMR spectrum using DMSO-d_6 solvent in a Bruker 400 MHz. ^{13}C NMR spectrum was also recorded for the ligand using a Bruker 100 MHz.

Thermal Analysis

Thermogravimetric Analysis (TGA)

Thermal stability of the ligand and its polychelates were determined using a thermogravimetric analyzer (Model SDT Q600) at a heating rate of 10°C/min in a static nitrogen atmosphere. On the basis of the results, the degradation pattern was proposed. The activation energy was calculated by the Freeman-Carroll method [19].

$$\frac{\Delta\log(dw/dt)}{\Delta\log Wr} = \frac{-Ea}{2.303R}\left\langle\frac{\Delta(1/T)}{\Delta\log Wr}\right\rangle + n$$

where, dw/dt is the rate of change of weight with time; $W_r = W_c - W$, where W_c is the weight loss at the completion of reaction or at definite time and W is the total weight loss up to time t; n is the order of reaction, T and R are the temperature and the gas constant, respectively.

Hence, a plot of $\Delta\log(dw/dt)/\Delta\log W_r$ vs. $\Delta(1/T)/\Delta\log W_r$ give an intercept on the y-axis equal to n and the slope is equal to $-E_a/2.303\,R$.

Differential Scanning Calorimetry (DSC)

The DSC thermogram was recorded using a thermogravimetric analyzer (Model SDT Q600) at a heating rate of 10°C/min in a static nitrogen atmosphere. The glass transition temperature (Tg) for the QAF ligand and its polychelates was determined.

SEM Studies

Scanning electron microscopic technique provides very useful information about the surface characteristics of any material. The surface morphology was investigated by a Hitachi (Model S-3000H) scanning electron microscope for QAF ligand and its polychelates at different magnifications.

Antimicrobial Screening

Biological assay depends upon a comparison of the inhibition of growth of microorganism by measuring the concentration of the sample to be examined with the known concentration of standard antibiotic. For the antimicrobial analysis the in vitro disc diffusion method has been employed. In this study the ligand and their chelates were tested for their effect on certain human pathogenic bacteria such as Gram-positive (*Staphylococcus aureus*), Gram-negative (*Escherichia coli*), and fungi (*Aspergillus niger and Candida albicans*).

The nutrient agar medium was boiled and sterilized by autoclaving at 7 kg pressure (121°C) for 15 min for the study of antibacterial activity. 20 mL media was poured into the sterilized petri plates and kept at room temperature for a few minutes, and allowed to solidify in plates. It was then incubated for 12 h and inoculated with microorganisms using sterile swabs. All of these manipulations were carried out with utmost care under aseptic conditions. The test solution prepared by dissolving the compounds in DMSO was filled with the media using a micropipette and incubated at 35°C for 48 h. The same procedure was adopted for the antifungal studies in which potato dextrose agar was the medium.

During the course of time, the test solution diffuses and the growth of the inoculated microorganisms such as *Staphylococcus aureus, Escherichia coli, Aspergillus niger*, and *Candida albicans* were found to be affected. The activity developed on the plate was measured by measuring the diameter of the inhibited zone in millimeters. The drug ciprofloxacin was used as the standard for bacteria and nystatin for fungi.

Electrical Conductivity Measurements

The electrical conductivity of the QAF ligand and its polychelates was measured using a Yokogawa 7651 instrument with a nickel sheet as a blank substrate and the polymer in DMSO solvent by the four-point method at a current rate of 5 amperes per second. The electrical properties were measured at various concentrations such as 0.05, 0.2, 0.4, and 0.6 mM and temperatures ranging from 50 to 100°C.

RESULTS AND DISCUSSION

The terpolymer ligand and its polychelates was soluble in solvents like N,N-dimethyl formamide (DMF), tetrahydrofuran (THF), and dimethyl sulphoxide (DMSO). Further, the ligand was also soluble in aqueous sodium and potassium hydroxide solutions. The physical and analytical data of the ligand and its polychelates are presented in Table 1. From the table, it is clear that the molecular formula of the terpolymer ligand and its polychelates are found to be in good agreement with the calculated values of C, H, N, and M. The amount of metal ion present in the polychelates indicates 1:2 (metal/ligand) stoichiometry and suggests that the formations of polychelates are resulting from the four ligand coordination and two water molecules coordination leading to the octahedral geometry. Hence, the general molecular formula for the QAF terpolymer ligand is $C_{17}H_{12}N_2O_3$ and for the polychelates is $C_{34}H_{22}N_4O_6M.2H_2O$.

Spectral Analysis

FTIR Spectra

FTIR is perhaps the most powerful tool for identifying the types of chemical bonds and functional groups. The FTIR spectrum of QAF ligand and its polychelates are depicted in Figure 1 and the frequency data are presented in Table 2. In the ligand spectrum, a broad band appeared in the region of 3442.8 cm^{-1} is assigned to the hydroxyl group of –COOH present in the aromatic ring [20]. This band seems to be merged with the band that appeared for the hydroxyl group of 8-hydroxyquinoline. A peak appeared at 2851.1 cm^{-1} and is assigned to the aromatic ring stretching modes [20] and a strong band at 1287.3 cm^{-1} is due to C–N stretching of the Ar-NH_2 group [21]. The 1,2,3,5 tetra substitution of the aromatic benzene ring by sharp, medium/weak absorption bands appeared between 1200 cm^{-1} and 800 cm^{-1}

Table 1: Physical and analytical data of the QAF ligand and its polychelates.

Compound	Empirical formula of the repeating unit	Formula mass of the repeating unit	Color	Yield (%)	Elemental Analysis (%)			
					Found (calcd.)			
					C	H	N	M
Ligand (QAF)	$C_{17}H_{12}N_2O_3$	294.1	Brown	85	70.81 (70.97)	5.55 (5.81)	8.71 (8.96)	–
$(CuL(H_2O)_2)_n$	$Cu{:}C_{34}H_{22}N_4O_6.2H_2O$	682.11	Dark brown	79	58.21 (59.01)	4.40 (4.54)	7.12 (7.33)	16.25 (16.31)
$(NiL(H_2O)_2)_n$	$Ni{:}C_{34}H_{22}N_4O_6.2H_2O$	677.26	Brown	82	60.01 (60.06)	4.41 (4.55)	7.44 (7.56)	14.99 (15.12)
$(ZnL(H_2O)_2)_n$	$Zn{:}C_{34}H_{22}N_4O_6.2H_2O$	683.96	Brown	77	58.91 (59.03)	4.19 (4.27)	7.12 (7.32)	16.25 (16.35)
$(PbL(H_2O)_2)_n$	$Pb{:}C_{34}H_{22}N_4O_6.2H_2O$	825.77	Brown	80	44.25 (44.31)	3.15 (3.24)	5.11 (5.21)	38.65 (38.95)

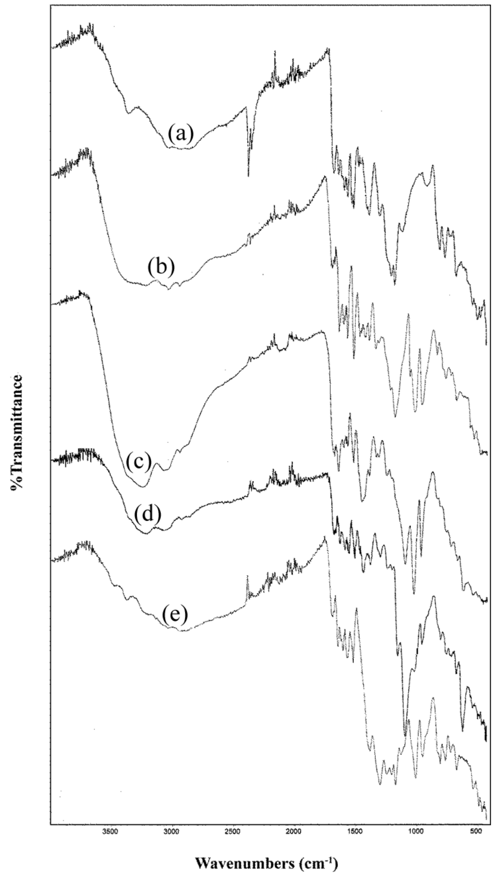

Figure 1: FTIR spectra of (a) QAF ligand, (b) QAF-Cu(II), (c) QAF-Ni(II), (d) QAF-Zn(II), and (e) QAF-Pb(II).

[22]. The band appearing at 1664.3 cm^{-1} is due to −C=O (carboxylic ketone) stretching vibrations [20]. A weak band appearing in the region 3031.1 cm^{-1} is attributed to $-CH_2$ linkage present in the terpolymer ligand [23]. This band

Table 2: FTIR spectral data of the QAF ligand and its polychelates.

	Observed frequencies (cm^{-1})						
Compound	ν **−OH**	ν **C−N (aromatic)**	ν **C=O**	ν **$-CH_2-$**	ν **C−O−M**	ν **M−O**	ν **C−N (8HQ)**
Ligand (QAF)	3412	1287	1664	3031	–	–	1577
$(CuL(H_2O)_2)_n$	3443	1292	1676	3004	1069	523	1550
$(NiL(H_2O)_2)_n$	3421	1314	1623	3055	1078	510	1500
$(ZnL(H_2O)_2)_n$	3440	1293	1655	3040	1076	536	1577
$PbL(H_2O)_2)_n$	3444	1285	1664	3055	1109	533	1583

seems to be merged with the band appearing for stretching modes of the aromatic ring. The band at 1664.3 – 1460.2 $\mathrm{cm^{-1}}$ may be assigned to C=N stretching vibrations of the heterocyclic ring and C=C stretching vibrations of the aromatic ring, respectively [24].

In the spectra of polychelates, a broad band appearing compared to its ligand in the region of 3300 $\mathrm{cm^{-1}}$ to 3600 $\mathrm{cm^{-1}}$ is due to the coordination of the ligand with the metal ions through the oxygen atom of phenolic group of 8-hydroxyquinoline and may also be due to the coordination of water molecules. A strong band that appeared at 1570 – 1585 $\mathrm{cm^{-1}}$ is assigned to the C-N stretching vibration of 8-hydroxyquinoline group and weak band that appeared in the region of 1070 – 1110 $\mathrm{cm^{-1}}$ are assigned to C–O–M stretching vibrations. The band ranges from 650 – 750 $\mathrm{cm^{-1}}$ are due to C–N stretching vibrations of the polychelates. The bands in the range of 500 – 530 $\mathrm{cm^{-1}}$ are is assigned to the M–O bond in the respective polychelates [24].

Electronic Spectra and Magnetic Moments

The electronic spectra provide more information about the electronic structure of the ligand and polychelates. Clear evidence is observed from the electronic absorption spectra of the QAF terpolymer ligand and its polychelates (Figure 2). The electronic spectra of all the polychelates exhibited different bands in the region 250–300 nm and 450–490 nm. The band appearing in the range of 250–300 nm is assigned as $\pi \rightarrow \pi^*$ transition of the ligand, whereas the band at 450–490 nm is assigned to polychelates, which clearly establishes the metal ion coordination with the oxygen and nitrogen atom present in the quinoline ring. The Zn-QAF polychelate is diamagnetic as expected, whereas the polychelates of Cu(II), Ni(II) are paramagnetic. The electronic spectra of Cu-QAF polychelate exhibit absorption at 28961 $\mathrm{cm^{-1}}$

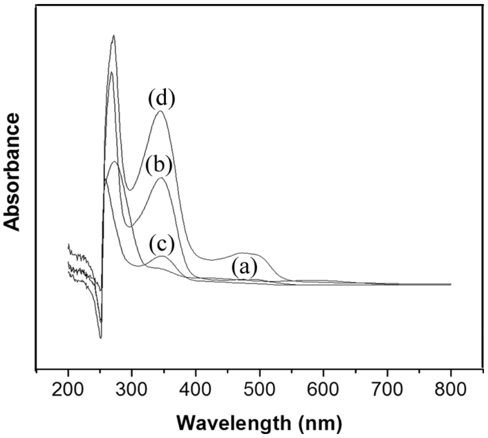

Figure 2: UV-vis spectra of (a) QAF ligand, (b) QAF-Cu(II), (c) QAF-Ni(II), and (d) QAF-Zn(II).

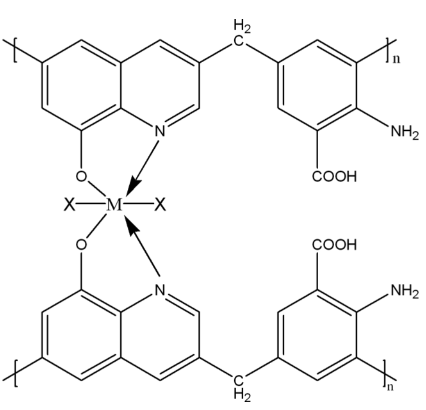

Figure 3: Proposed structure of the polychelates.

due to the charge transfer transition, and the transition that occurs at 16949 cm^{-1} is assigned as $^2E_g \rightarrow {}^2T_{2g}$ in an octahedral environment with a magnetic moment of 1.73 BM. Bands observed at 28968 and 20772 cm^{-1} are is assigned as $^3A_{2g} \rightarrow {}^3T_{1g}(P)$ and $^3A_{2g}(P) \rightarrow {}^3T_{1g}(F)$ for Ni-QAF polychelate with octahedral geometry, and the magnetic moment is found to be 3.24 BM. Based on the above studies, the geometry of the polychelates is proposed (Figure 3).

NMR Spectra

The ^1H NMR spectrum of the QAF terpolymer ligand and its polychelates are shown in Figure 4 and the spectral data are presented in Table 3. The signal at 8.78 ppm is assigned to the $-OH$ of Ar$-$COOH and this downfield shift is due to the intramolecular hydrogen bonding between $-OH$ of Ar-COOH and the proton of $-NH_2$ of Ar$-NH_2$ group [23]. The signals in the region of 7.2–7.8 ppm are assigned to all the protons of the aromatic ring [22]. The signals appearing in the region of 2.49 to 4.70 ppm are due to the methylene proton of the Ar$-CH_2$ bridge [20]. The signal obtained at 9.1 ppm is attributed to the $-OH$ of quinoline ring [20].

The ^{13}C NMR spectrum of the QAF ligand is shown in Figure 5. The observed chemical shifts are assigned on the basis of the literature [20, 25]. The spectrum shows the corresponding peaks at 110.4, 146.3, 128.3, 134.9, 126.2, and 128.3 ppm with respect to C_1 to C_6 of the amino aromatic ring. The peak appeared at 43.2 ppm is assigned to the Ar–CH_2 bridge in the ligand. The peaks corresponding to C_1 to C_9 of the quinoline ring appeared at 150.4, 134.6, 133.6, 128.3, 117.9, 134.9, 110.4, 148.9, and 150.4 ppm, respectively, in the ligand.

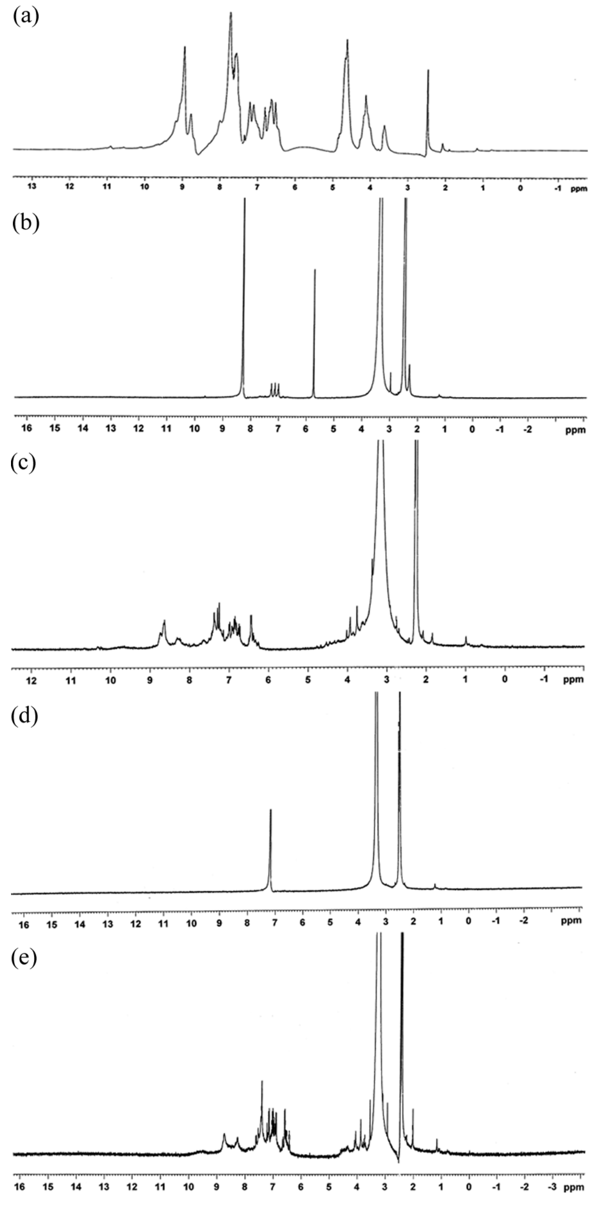

Figure 4: ^{1}H NMR spectra of (a) QAF ligand, (b) QAF-Cu(II), (c) QAF-Ni(II), (d) QAF-Zn(II), and (e) QAF-Pb(II).

The ^{1}H NMR spectra of all the polychelates show multiplets in the range of 6.8–8.4 ppm and are assigned to the aromatic protons. The signals observed in the region 2.02–4.23 ppm are due to the methylene protons. The signal obtained at 9.1 ppm is assigned to $-$OH of quinoline ring in the polymeric ligand and is completely disappeared in the case of polychelates, which is clear

Table 3: ^{1}H-NMR spectral data of the QAF ligand and its polychelates.

Compound	Chemical shifts (ppm) Aromatic Protons	−OH of −COOH group involved intramolecular hydrogen bonding	Ar−CH_2 moiety	−OH of quinoline ring
Ligand (QAF)	7.2–7.8	8.78	2.49–4.70	9.1
$(CuL(H_2O)_2)_n$	6.8–8.4	8.74	2.44–4.10	–
$(NiL(H_2O)_2)_n$	6.5–7.8	8.75	2.02–4.09	–
$(ZnL(H_2O)_2)_n$	7.1–7.5	8.57	2.02–4.10	–
$(PbL(H_2O)_2)_n$	7.1–7.5	8.61	2.06–4.23	–

evidence for the bond formation of metal ion with the ligand through the oxygen atom of the −OH group in the quinoline ring. Based on the data obtained from FTIR, electronic absorption, and NMR (^{1}H and ^{13}C), the structure of the ligand and the polychelates is proposed.

Thermal Analysis

TGA Measurements

The thermogravimetric analysis is a method to compare the thermal stability of the polymeric ligand and its chelates. The QAF ligand exhibits three stage of degradation. The first degradation stage ranges from 180 to 250°C which corresponds to the loss of −COOH group as CO_2 [19]. The second degradation ranges from 250 to 480°C and may be due to the elimination of the amino aromatic ring. Finally the third degradation stage takes place between 500 to 900°C and may be the complete degradation of the polymer. The higher degradation temperature of the terpolymer is due to the strong intramolecular

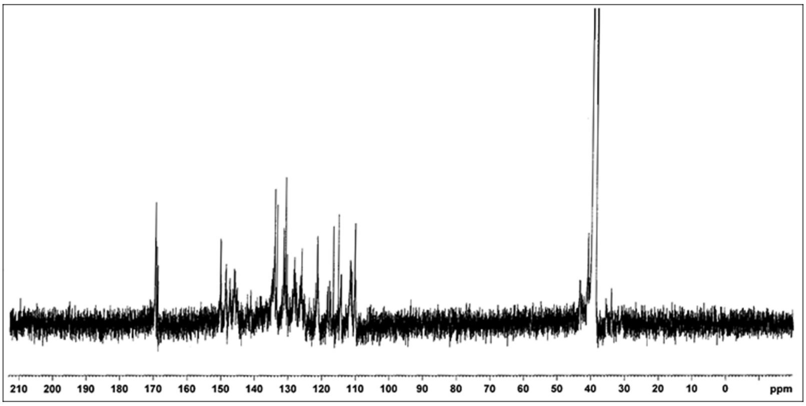

Figure 5: ^{13}C-NMR spectra of the ligand.

hydrogen bonding established in the amino aromatic ring [14]. The proposed scheme for the thermal degradation of the ligand may be assigned as follows:

$$\text{i)}\quad [\text{QAF}]_n.\ n\text{H}_2\text{O} \xrightarrow[\text{50 °C to 110 °C}]{\text{loss of moisture}} [\text{QAF}]_n + n\text{H}_2\text{O}$$

$$\text{ii)}\quad [\text{QAF}]_n \xrightarrow[\text{150 °C to 250 °C}]{} [\text{QAF}]_n + \text{loss of -COOH from aromatic ring}$$

$$\text{iii)}\quad [\text{QAF}]_n \xrightarrow[\text{250 °C to 500 °C}]{} \text{8Q} + \text{loss of amino aromatic ring}$$

$$\text{iv)}\quad \text{8Q} \xrightarrow[\text{500 °C to 910 °C}]{} \text{93.6 \% of weight loss of resin}$$

The thermal degradation of the polychelates involves a two step processes. The initial weight loss is due to the elimination of hydrated water in the polymeric chelates. The first degradation stage ranges from 150 to 300°C and may be due to the removal of coordinated water molecules in the chelates. The second degradation stage ranges from 350 to 850°C in which the noncoordinated part of the ligand decomposes first, while the coordinated part decomposes later. Further, both the ligand and the polychelates possess a similar range of thermal stability, and this may be due to the intramolecular hydrogen bonding in the ligand and its chelates which is undisturbed. On the basis of the TG data, the thermal stability of the ligand is found to be higher than that of its polychelates, because the metal ions in the chelates might have developed a considerable strain in the ring. The thermal stability of the Cu-QAF chelate is found to be higher than the other chelates such as Zn-QAF, Pb-QAF, and Ni-QAF under study. The thermal stability of QAF ligand and its polychelates is found to be very high when compared to the other polychelates reported in the earlier literature [12,23]. The proposed scheme of thermal degradation of the polychelates is as follows:

$$\text{i)}\quad [\text{ML}(\text{H}_2\text{O})_2]_n.\ n\text{H}_2\text{O} \xrightarrow[\text{50 °C to 110 °C}]{\text{loss of moisture}} [\text{ML}(\text{H}_2\text{O})_2]_n + n\text{H}_2\text{O}$$

$$\text{ii)}\quad [\text{ML}(\text{H}_2\text{O})_2]_n \xrightarrow[\text{150 °C to 300 °C}]{\text{loss of coordinated water molecules}} [\text{ML}]_n + 2\text{H}_2\text{O}$$

$$\text{iii)}\quad [\text{ML}]_n \xrightarrow[\text{350 °C to 850 °C}]{} \text{Metal oxide}$$

The TG data and the activation energy calculated by the Freeman-Carroll method for both the ligand and its polychelates formation are given in the Table 4 and the thermograms are shown in Figure 6. The order of the thermal stability are found to be QAF ligand > Cu-QAF > Zn-QAF > Pb-QAF > Ni-QAF.

Table 4: Thermogravimetric data of QAF ligand and its polychelates.

	Percentage (%) weight loss at various temperature (°C)										
Compound	**250**	**350**	**450**	**550**	**650**	**750**	**850**	**950**	**T_{max}* (°C)**	**T_{50}** (°C)**	**Activation energy (E_a) kJ mol^{-1}**
Ligand (QAF)	25.7	38.9	59.7	64.7	71.0	80.9	90.0	96.4	908.7	401.0	20.23
$(CuL(H_2O)_2)_n$	33.7	44.8	51.9	56.8	62.9	74.0	87.0	93.1	890.2	420.8	19.21
$(NiL(H_2O)_2)_n$	36.1	44.7	49.0	60.4	77.1	89.0	90.4	–	776.8	466.7	16.62
$(ZnL(H_2O)_2)_n$	20.3	31.2	35.6	43.2	58.1	76.3	92.0	–	865.1	604.4	17.36
$(PbL(H_2O)_2)_n$	25.3	31.3	38.4	65.6	81.7	84.3	91.1	–	784.7	504.5	19.98

*Maximum decomposition temperature; **Temperature of 50% weight loss.

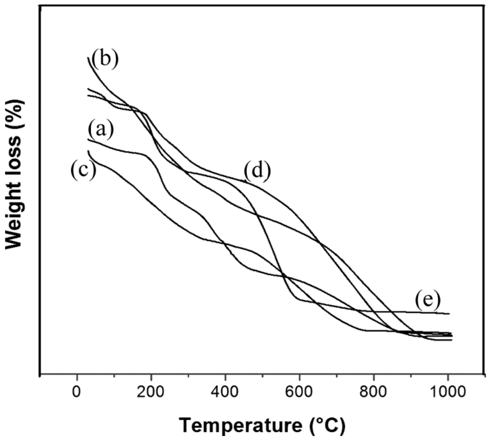

Figure 6: TGA thermograms of (a) QAF ligand, (b) QAF-Cu(II), (c) QAF-Ni(II), (d) QAF-Zn(II), and (e) QAF-Pb(II).

DSC Measurements

The DSC thermograms of the QAF terpolymer ligand and its polychelates are illustrated in Figure 7. From the DSC measurements, Tg was taken as the midpoint of the transition region. The ligand shows a single Tg value of 109.2°C. All the polychelates showed an increased glass transition temperature compared to the ligand. The glass transition temperature of QAF-Cu, QAF-Ni, QAF-Zn, and QAF-Pb polychelates are found to be 136.7, 154.4, 127.1, and 127.4°C, respectively. The higher Tg values for the polychelates are due to the decrease in the segmental mobility as a result of anchoring the metal ions between the polymer chains. The DSC thermogram of the QAF ligand and its polychelates indicates a characteristic endothermic transition which corresponds to the evolution of water (moisture). This transition is consistent with the first observation in the initial weight loss from the TGA.

SEM and Molecular Weight Measurements

The morphology of the QAF terpolymer ligand shows deep pits and a less close-packed surface. The SEM image also reveals that the terpolymer ligand is highly porous. However, the polychelates show stiff and close-packed morphology, which is quite different from that of its ligand (Figure 8). The increased close packing in the case of polychelates is due to the incorporation of metal ions. An ice rock shape is observed in the case of QAF-Cu with the particle size of 10 μm. A single crystal-like structure for QAF-Ni, cloud-shaped for QAF-Zn and crystals accumulated structure for QAF-Pb are observed with

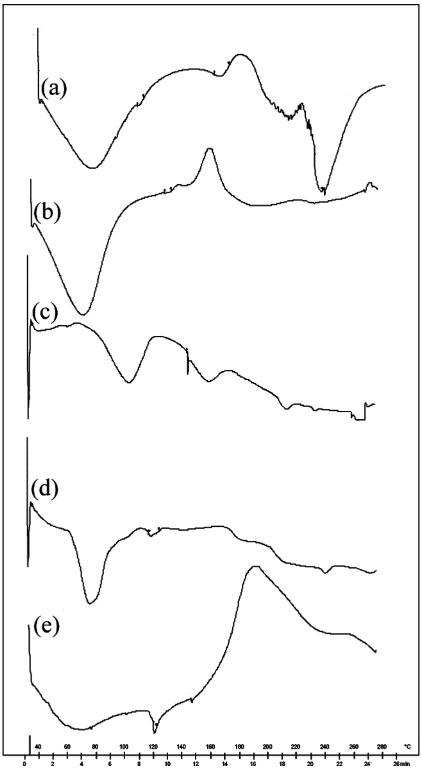

Figure 7: DSC thermograms of (a) QAF ligand, (b) QAF-Cu(II), (c) QAF-Ni(II), (d) QAF-Zn(II), and (e) QAF-Pb(II).

the particle size almost equal to 1 μm. The viscosity-average molecular weight of the terpolymer is found to be 3200.

Antimicrobial Screening

The microbial screening results of the QAF terpolymer ligand and its polychelates are presented in Table 5. Compared to the ligand, the polychelates show higher activity is due to the metal ions shared with the donor atoms of the ligand and the π-electron delocalization over the whole chelate ring. This effect increases the lipophilic character of the metal ion, which favors the permeation through the lipoid layers of the bacterial and fungal membranes [26]. The higher activity may also be due to the presence of $-OH$ and the aromatic ring [27]. It is perceived that the factors such as solubility, conductivity, dipole moment and cell permeability mechanism may be alternative reasons for the increased activity of the metal complexes [28]. Both the ligand and polychelates have good inhibition against the growth of Gram-negative bacteria which

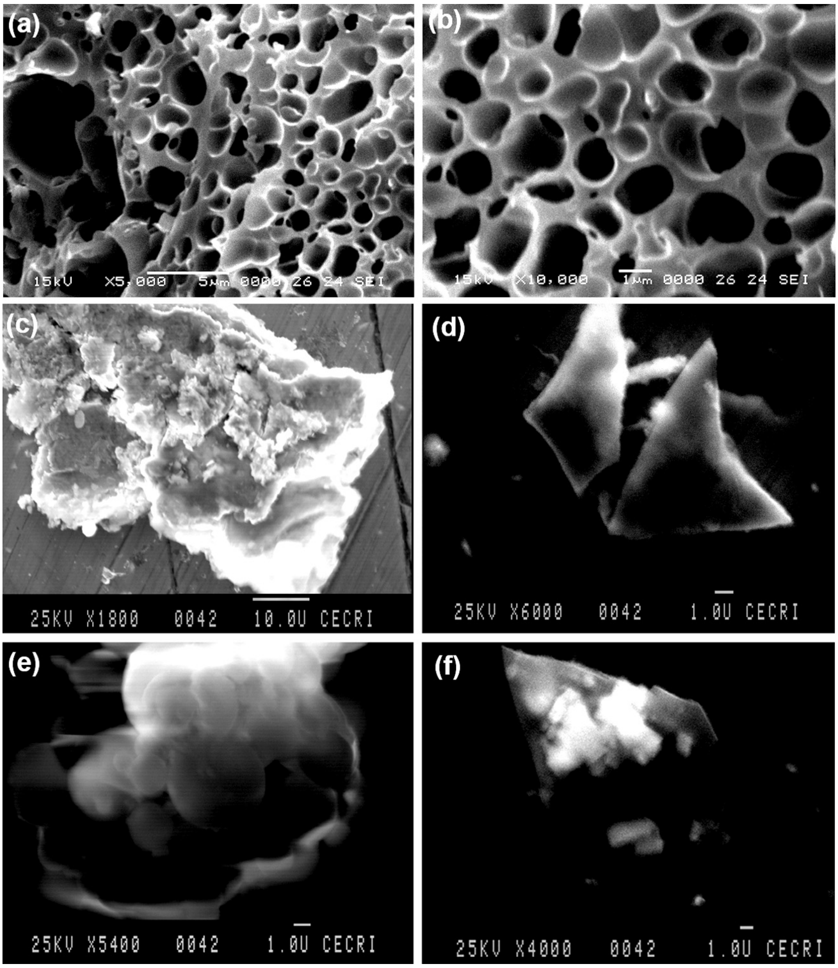

Figure 8: SEM images of (a) and (b) QAF ligand, (c) QAF-Cu(II), (d) QAF-Ni(II), (e) QAF-Zn(II), and (f) QAF-Pb(II).

Table 5: Antimicrobial activities of QAF ligand and its polychelates.

	Diameter of zone of inhibition (mm)			
Compound	***S. Aureus***	***E. Coli***	***A. Niger***	***C. Albicans***
Ligand (QAF)	++	+++	+++	++
$(CuL(H_2O)_2)_n$	+++	++++	+++++	++++
$(NiL(H_2O)_2)_n$	+++	++++	++++	+++
$(ZnL(H_2O)_2)_n$	+++	++++	+++	+++
$(PbL(H_2O)_2)_n$	+++	+++	+++	++
Solvent (DMSO)	–	–	–	–

Standard (Ciprofloxacin –5 µg for bacteria, Nystatin-10 µg for fungi); % inhibition: + (10–25%), ++ (26–40%), +++ (41–55%), ++++ (56–70%), +++++ (71–85%), ++++++ (86–100%).

Table 6: Electrical conductivity of QAF ligand and its polychelates at various concentrations.

	Concentrations (mM)			
	0.05	0.20	0.40	0.60
Compound	Conductivity (mho m^{-1}) × 10^{-1}			
Ligand (QAF)	1.47	1.35	1.24	1.16
$(CuL(H_2O)_2)_n$	2.86	2.28	1.82	1.45
$(NiL(H_2O)_2)_n$	2.48	1.98	1.58	1.26
$(ZnL(H_2O)_2)_n$	2.45	1.96	1.54	1.23
$(PbL(H_2O)_2)_n$	1.94	1.55	1.32	1.20

induces tumor. Hence the polychelates and ligand may possess antitumor activity. The Gram-positive bacteria are both pathogenic and invasive. The polychelates have good inhibition characteristics against the growth of this pathogen. *Aspergillus niger* cause aspergillosis, the growth of the fungus is controlled by the terpolymer chelates to some extent. The *Candida albicans* can penetrate into the intestinal walls and cause diseases. From the findings, the growth of *Candida albicans* is inhibited by the addition of QAF polymer chelates.

Electrical Conductivity Measurements

The electrical conductivity of the QAF ligand is 1.47×10^{-1} mho m^{-1} at 0.05 mM and decreases as the concentration increases (Table 6). Further, the conductivity of the ligand decreases on increasing the temperature (Table 7). This trend is very similar to the metallic conductors. It is also suggested that the decrease in conductivity is due to the elimination of the adsorbed or absorbed gases or solvent traces present in the ligand. The order of electrical conductivity of the ligand and its polychelates are Cu-QAF > Ni-QAF > Zn-QAF > Pb-QAF > QAF ligand.

Table 7: Electrical conductivity of QAF ligand and its polychelates at various temperatures.

	Temperatures (°C)					
	50	60	70	80	90	100
Compound	Conductivity (mho m^{-1}) × 10^{-1}					
Ligand (QAF)	1.33	1.31	1.05	0.78	0.67	0.53
$(CuL(H_2O)_2)_n$	2.51	2.02	1.60	1.28	1.02	0.81
$(NiL(H_2O)_2)_n$	2.33	1.86	1.48	1.18	0.94	0.75
$(ZnL(H_2O)_2)_n$	2.15	1.72	1.37	1.10	0.88	0.71
$(PbL(H_2O)_2)_n$	1.65	1.32	1.20	0.84	0.77	0.65

CONCLUSION

Polychelates prepared using a terpolymer ligand derived from 8-hydroxyquinoline and anthranilic acid with formaldehyde with specific metal ions are thermally stable. The viscosity-average molecular weight of the terpolymer is found to be 3200. Incorporation of the metal ions into the polymer matrix fills the voids and gaps to make the polychelates more closely packed. The polychelates show higher activity against certain bacterial strains such as *Staphylococcus aureus, Escherichia coli*, and fungal strains *Aspergillus niger* and *Candida albicans*.

REFERENCES

[1] Draye, M., and Czerwinski, K. R. *Sep. Sci. Technol.* **35**, 1117 (2000).

[2] Burkanudeen, A., and Karunakaran, M. *Orient. J. Chem.* **19**, 225 (2003).

[3] Patel, S. A., Shah, B. S., and Patel, R. M. *Iran. Polym. J.* **13**, 445 (2004).

[4] Karunakaran, M., and Burkanudeen, A. *Orient. J. Chem.* **18**, 65 (2002).

[5] Ismail, A. I., Ebraheem, K. A. K., Mubarak, M. S., and Khalili, F. I. *Solvent Extr. Ion. Exch.* **21**, 125 (2003).

[6] Rivas, B. L., and Seguel, G. V. *Polyhedron* **18**, 2511 (1999).

[7] Mart, H., and Vilayetgloglu, A. R. *Polym. Degrad. Stab.* **83**, 255 (2004).

[8] Nanjundan, S., Selvamalar, C. S. J., and Jayakumar, R. *Eur. Polym. J.* **40**, 2313 (2004).

[9] Sathisha, M. P., Shetti, U. N., Revankar, V. K., and Pai, K. S. R. *Eur. J. Med. Chem.* **43**, 2338 (2008).

[10] Mahmoud, M. E., Haggag, S. S., and Fattah, T. M. A. *Polyhedron* **28**, 181 (2009).

[11] Rivas, B. L., Seguel, G. V., and Ancatripai, C. *Polym. Bull.* **44**, 445 (2000).

[12] Kapadia, M., Patel, M., Patel, G., and Joshi, J. *J. Polym. Res.* **15**, 285 (2008).

[13] Thamizharasi, S., Reddy, A. V. R., and Balasubramanian S. *React. Funct. Polym.* **40**, 143 (1999).

[14] Patel, M. M., Kapadia, M. A., and Joshi, D. D. *Polym. Int.* **58**, 728 (2009).

[15] Ukey, V. V., and Juneja, H. D. *J. Appl. Polym. Sci.* **99**, 273 (2006).

[16] Warawsky, A., Wang, Y., and Berkowitzm, B. *Sep. Sci. Technol.* **38**, 149 (2003).

[17] Kavlak, S., Can, H. K., Rzaev, Z. M. O., and Guner, A. *J. Appl. Polym. Sci.* **100**, 3926 (2006).

[18] Patel, M. B., Patel, S. A., Ray, A., and Patel, R. M. *J. Appl. Polym. Sci.* **89**, 895 (2003).

[19] Azarudeen, R. S., Riswan Ahamed, M. A., Jeyakumar, D., and Burkanudeen, A. R. *Iran. Polym. J.* **18**, 821 (2009).

[20] Silverstein, R. M., and Webster, F. X. (1998). *Spectrometric Identification of Organic Compounds*, 6th Ed. John Wiley & Sons, Inc., New York, p. 217.

[21] Raj, J. A., Vedhi, C., Burkanudeen, A., Arumugam, P., and Manisankar, P. *Ionics* **16**, 171 (2010).

[22] Nakanishi, K. (1967). *Infra Red Absorption Spectroscopy Practical*. Golden Day, Inc and Nankoda Co. Ltd., Tokyo.

[23] Singru, R. N., Zade, A. B., and Gurunule, W. B. *J. Appl. Polym. Sci.* **109**, 859 (2008).

[24] Shah, T. B., Dixit, R. B., and Dixit, B. C. *J. Therm. Anal. Cal.* **92**, 505 (2008).

[25] Pretsch, E., Buhlmann, P., and Affolter, C. (2000). *Structure Determination of Organic Compounds*. Springer-Verlag Berlin Heidelberg, New York.

[26] Patel, M. M., Kapadia, M. A., Patel, G. P., and Joshi, J. D. *J. Appl. Polym. Sci.* **106**, 1307 (2007).

[27] Singh, N., Gupta, S., and Nath, G. *Central National De La Recherche Scientifique (CAT. INIST)* **14**, 484 (2000).

[28] Bagihalli, G. B., Patil, S. A., and Badami, P. S. *J. Iran. Chem. Soc.* **6** (2), 259 (2009).